Structure of the mixed-valence platinum complexes $[Pt^{II}(en)(SCN)_2][Pt^{IV}(en)(SCN)_2I_2]$ and *cis*-$[Pt^{II}(NH_3)_2(SCN)_2][Pt^{IV}(NH_3)_2(SCN)_2I_2]$ studied by the method of radial distribution functions of atoms

V. I. Korsunsky*

Institute of Chemical Kinetics and Combustion, Siberian Branch of the U.S.S.R. Academy of Sciences, Novosibirsk 630090 (U.S.S.R.)

G. S. Muraveiskaya and A. A. Sidorov

N. S. Kurnakov Institute of General and Inorganic Chemistry of the U.S.S.R. Academy of Sciences, Moscow (U.S.S.R.)

(Received February 11, 1991)

Abstract

Using the method of radial distribution functions of atoms obtained by Fourier transform of powder X-ray patterns it has been shown directly that the structures of the mixed-valence complexes *cis*-$[Pt^{II}(NH_3)_2(SCN)_2][Pt^{IV}(NH_3)_2(SCN)_2I_2]$ (**I**) and $[Pt^{II}(en)(SCN)_2][Pt^{IV}(en)(SCN)_2I_2]$ (**II**) (en = ethylenediamine) contain the linear chains ...I–Pt^{IV}–I...Pt^{II}...I–Pt^{IV}–I...Pt^{II}...I–, wherein square-planar complexes of Pt^{II} alternate with octahedral complexes of Pt^{IV}. Such a structure for **I** had earlier been proposed only on the basis of indirect spectroscopical data. The distances Pt^{IV}–I and Pt^{II}...I have been determined. The first one is 2.70 Å in both the complexes and the second is 3.50 Å in **I** and 3.23 Å in **II**. The distances Pt^{II}...I are considerably longer than corresponding distances in the similar mixed-valence complex of known structure $[Pt^{II}(en)_2][Pt^{IV}(en)_2I_2](ClO_4)_4$ (**IV**) (about 3.10 Å). The elongation of the Pt^{II}...I contact corresponds to the smaller bridge role of I atoms in the thiocianate complexes, to the smaller electron delocalization over the chain of Pt and I atoms and, hence, to a more pronounced division of the system into true complexes of Pt^{II} and Pt^{IV} than in **IV**.

Introduction

As long ago as in 1968 [1], by means of oxidation of *cis*-dithiocyanatodiammine platinum(II) by iodine, one of the authors had obtained the compound $(NH_3)_2(SCN)_2PtI$ formally containing platinum in the oxidation state 3+. Later, having studied the electronic, IR and resonance Raman spectra of this complex and having found these spectra to be analogous to those of the complexes with known structure $[Pt^{II}(en)_2][Pt^{IV}(en)_2I_2](ClO_4)_4$ and $[Pt^{II}(en)I_2]$-$[Pt^{IV}(en)I_4]$, Clark and coworkers [2, 3] attributed the rhodanide complex to mixed-valence compounds: *cis*-$[Pt^{II}(NH_3)_2(SCN)_2][Pt^{IV}(NH_3)_2(SCN)_2I_2]$ [2, 3]. It was assumed that, as in the mentioned ethylenediamine analogs, altering square-planar Pt^{II} and octahedral Pt^{IV} complexes were arranged so that platinum and iodine atoms formed linear chains ...I–Pt^{IV}–I...Pt^{II}...I–Pt^{IV}–I...Pt^{II}...I–, with iodine atoms being bridges between platinum atoms. However, since one failed to grow single crystals for X-ray analysis, no direct structural corroboration of this assumption has been obtained. Spectral data provide only very indirect evidence for the described structure. Therefore, we have investigated compounds of such a type with the use of novel, more direct, ways of studying their structural parameters in powder samples.

By way of a large number of examples it has been recently shown (see, for example, refs. 4–8) that in the case of polynuclear complexes containing heavy atoms and when a substance is available only as a powder, the method of radial distribution functions (RDF) of atoms, being obtained by Fourier-transform of powder X-ray patterns [9, 10], is fruitful for the solution of structural problems. The RDF $G(r)$ is the spectrum of interatomic distances of a powder (polycrystalline or amorphous). Each interatomic distance corresponds to a contribution to the $G(r)$ in the form of a peak at an argument r equal to

*Author to whom correspondence should be addressed.

0020-1693/91/$3.50

this distance. The peak intensity is approximately proportional to the product of the numbers of electrons in the pair of atoms inducing the peak. As a result, the peaks corresponding to distances between heavy atoms usually give the dominant contribution to RDF. One can quite simply and unambiguously identify such peaks, and their positions yield, in the first approximation, the values of corresponding distances, particularly if both atoms are heavy.

Of special importance is the fact that the peak intensity for a given type of distances is also proportional to the number of such distances. The contribution of one distance between atoms of given types in a pair can be calculated exactly. This makes it possible to construct trial structural models of a complex with specified interatomic distances and, taking into account their numbers, to calculate a model spectrum of distances $G(r)$. Comparing such spectra of different models with an experimental spectrum, one can select an adequate structure. Mean interatomic distances r_{kj} and r.m.s. deviations from r_{kj} due to, for instance, atomic vibrations, σ_{kj}, are fitting parameters varied within reasonable limits. The numbers of distances between k- and j-type atoms, N_{kj}, (counted per stoichiometric unit) change discretely from one model to another and are invariable in fitting a model to experimental RDF. Thus, in terms of this technique, we deal with direct structural parameters of a compound. Direct data are obtained mainly on the arrangement of heavy atoms and often on essential features of the surroundings of heavy atoms with more light ligand atoms. The presence of heavy subsystem makes calculations much more simple and indeed informative since contributions of more numerous distances between light atoms to RDF may be ignored. First, when overlapping the peaks of several types of distances, these contributions, owing to their low level, do not mask the main information. Second, RDF simulation formulae contain a reasonable number of parameters. The general idea and real procedures of the RDF method application to the described problem have been reported in detail elsewhere [4, 5].

In this work, the RDF method is used for a direct structural study of two rhodanide complexes of the class under discussion: the abovementioned ammonia derivative (compound **I**) and its analog where both NH_3 ligands of Pt^{II} and Pt^{IV} are changed by NH_2 groups of ethylenediamine (compound **II**). The method allows direct detection and measurement of interatomic distances between heavy atoms of platinum and iodine, which are the basic parameters in verification of structural models. One also can check the correspondence between the numbers of these distances in the linear chain model ...I–Pt^{IV}–I...Pt^{II}...I–Pt^{IV}–I...Pt^{II}...I– and RDF peak intensities. Information about the types and amounts of ligands other than iodine in the synthesized compounds is obtained mainly from analyzing their IR spectra, synthesis procedure, and from chemical analysis data. Quantitative simulation of RDF profiles, with account of these data, allows one to obtain more detailed information on the structure of the studied compounds [4–8].

Experimental

Preparation of compounds

Synthesis procedures for the initial compounds have been described elsewhere (for *cis*-$[Pt(NH_3)_2(SCN)_2]$ and $[Pt(en)(SCN)_2]$ see ref. 11, for *cis*-$[Pt(NH_3)_2(SCN)_2Br_2]$ see ref. 12). The substances were identified by chemical analysis data, IR spectra (all bands typical for a certain compound have been assigned) and crystallooptical analysis of homogeneity. The complex $[Pt^{II}(en)_2][Pt^{IV}(en)_2I_2](ClO_4)_4$ which is a reference substance for the method of radial distribution functions was obtained by the procedure described previously [13].

cis-$[Pt(NH_3)_2(SCN)_2][Pt(NH_3)_2(SCN)_2I_2]$ (I)

This complex was obtained by the following two methods.

(1) Iodine dissolved in wetted tertiary butyl alcohol (TBA_{aq}) (approximately 1.5 equiv. per equiv. of initial salt) was added to a suspension of a weighed portion of *cis*-$[Pt(NH_3)_2(SCN)_2]$ (approximately 0.5 g) thoroughly ground in an agate mortar containing 20 to 25 ml of TBA_{aq} while being continuously stirred [1]. The resulted bronze–green precipitate was filtered off and washed with absolute TBA (TBA_{abs}) to remove iodine. The precipitate was dried in an exsiccator without vacuum treatment. *Anal.* Calc. for $[Pt(NH_3)_2(SCN)_2][Pt(NH_3)_2(SCN)_2I_2]$: Pt, 41.33; S, 13.61; N, 11.85; I, 26.87. Found: Pt, 41.38; S, 13.68; N, 11.85; I, 27.47%.

(2) Via interaction of equivalent amounts of *cis*-$[Pt(NH_3)_2(SCN)_2]$ and *cis*-$[Pt(NH_3)_2(SCN)_2I_2]$. Approximately 0.5 g of parent compounds taken in the 1:1 proportion was ground in an agate mortar containing 5 to 10 ml of TBA_{aq}. The resulted bronze–green precipitate was filtered in 15 to 20 min and washed with TBA_{abs}. *Anal.* Found: Pt, 41.25; S, 13.58; N, 11.89; I, 27.33%.

$[Pt(en)(SCN)_2][Pt(en)(SCN)_2I_2]$ (II)

25 ml of iodine solution in TBA_{abs} (two moles per mole of the initial salt) was added to 1.0 g of

fine $[Pt(en)(SCN)_2]$ suspended in 10 ml of TBA_{abs}. The reaction mixture was continuously stirred for 6 h in a closed vessel, then kept for a further 24 h. The obtained brown product $Pt(en)(SCN)_2I_{1.44}$ (Found: Pt, 35.23; S, 11.59; N, 10.60; I, 33.78%) is a mixture of partially non-iodinated $[Pt(en)(SCN)_2]$ and an unknown compound, probably, diiodide $[Pt(en)(SCN)_2I_2]$ according to the powder X-ray pattern. Further the product was introduced into the reaction with the parent $[Pt(en)(SCN)_2]$. To do this, 0.522 g of $Pt(en)(SCN)_2I_{1.44}$ was thoroughly ground in an agate mortar containing 0.112 g of $[Pt(en)(SCN)_2]$, i.e. the ingredients were taken in the proportion required for formation of $[Pt(en)(SCN)_2][Pt(en)(SCN)_2I_2]$. 0.5 to 1 ml of water or TBA_{aq} was added to the mixture which was then ground for several minutes more. The resulted bronze–green precipitate was transferred to a filter and dried without vacuum treatment. The powder X-ray pattern showed the parent components to be completely absent, i.e. the transformation is complete. *Anal.* Calc. for $[Pt(en)(SCN)_2][Pt(en)(SCN)_2I_2]$: Pt, 39.16; S, 12.87; N, 5.62. Found: Pt, 38.15; S, 12.89; N, 5.52%.

cis-$[Pt(NH_3)_2(SCN)_2I_2]$ (III)

This complex was obtained by the following two methods.

(1) Iodine dissolved in TBA_{abs} (not less than 2.5 equiv.) was added to the suspension of 0.5 g of *cis*-$[Pt(NH_3)_2(SCN)_2]$ in 5–10 ml of TBA_{abs}. The mixture was stirred in a closed vessel or dry chamber (to avoid ingress of water) for 6–8 h. The resulted violet–brown precipitate was washed on a filter with TBA_{abs} and dried without vacuum treatment. *Anal.* Calc. for $[Pt(NH_3)_2(SCN)_2I_2]$:Pt, 32.85; S, 10.68; N, 9.34; I, 42.36. Found: Pt, 33.01; S, 10.75; N, 9.63; I, 42.58%.

(2) 2.5 moles of KI dissolved in water were added to aqueous suspension of *cis*-$[Pt(NH_3)_2(SCN)_2Br_2]$. As a result, the orange–red precipitate immediately converted to the almost black precipitate of the diiodo derivative **III**. *Anal.* Found: Pt, 33.10; S, 10.33; N, 9.30; I, 42.33%.

The identity of products **I** and **III** obtained by the two different methods has been established from the IR spectra and powder X-ray patterns.

In the above syntheses, water plays an important role. No mixed-valence complexes **I** and **II** are formed in the absence of water. Participation of H_2O in chemical processes in the syntheses of mixed-valence compounds has already been suggested [14].

Physical measurements

IR spectra were recorded using Specord 75IR (400–4000 cm^{-1}) and Bruker IFS-113V (50–500 cm^{-1}) spectrometers. Samples – powders in vaseline oil, cell windows – KBr and polyethylene, respectively. ESR spectra were measured on a RE-1306 spectrometer at room temperature. Magnetic field was calibrated against the signal of paramagnetic Mn^{2+} ions diluted in MgO. X-ray photoelectron spectra (XPS) were detected on a VIEF-15 Varian spectrometer.

X-ray scattering measurements were made using a DRON-3M X-ray diffractometer. The procedure for measuring powder X-ray patterns suitable for RDF calculations and the main points of the calculation techniques utilized for obtaining experimental RDFs and RDFs of structural models have been described previously [4, 5]. Parameters of structural models for the investigated substances (Fig. 3) which are also coefficients in the model RDF calculation formulae from refs. 4, 5, are given in the captions to Figs. 1 and 2. All samples showed X-ray patterns typical of polycrystalline powders. X-ray scattering curves for RDF calculations were obtained with the use of monochromatic Ag Kα radiation at angles of diffraction up to $2\vartheta \approx 80$–$85°$ ($q_{max} = 4\pi \sin \vartheta_{max}/\lambda \approx 14.5$–$15$ $Å^{-1}$). For phase determination from powder X-ray patterns Cu Kα radiation was used.

Results and discussion

The major subject to be discussed in this section will be the RDFs of the complexes. However, structural models given later will be based indirectly on the conclusion following mainly from analysis of IR spectra: the arrangement of equatorial NH_3 and SCN ligands of platinum atoms is unchanged in all transformations of initial *cis*-$[Pt(NH_3)_2(SCN)_2]$. It follows from the fact that the IR spectra of iodine derivatives preserve absorption bands of all types of vibration – intraligand and those attributed to ligand bonding to Pt atoms in *cis*-$[Pt(NH_3)_2(SCN)_2]$ – with some shifts and, sometimes, splittings. The same conclusion is accepted for complex **II** originating from $[Pt^{II}(en)(SCN)_2]$, although in this case the spectrum of the initial compound is already more complex than the spectrum of the ammonia derivative and it is difficult to perform a complete assignment of the spectral bands. Nevertheless, the main spectral bands of the initial complex are observed in the spectrum of **II**, and this allows us to make such a conclusion. The RDFs of the compounds under discussion are in good agreement with the conclusions stated above, but radial functions are not a sensitive test for the details of possible rearrangements of light ligands. Such changes in ligand sphere of Pt may produce small changes in RDF.

Figure 1 shows RDFs (solid lines) for *cis*-$[Pt(NH_3)_2(SCN)_2]$ (bottom) and $[Pt(NH_3)_2(SCN)_2I_2]$ (top) whose molecules, as assumed [2, 3], in a 1:1 ratio form linear chains in the mixed-valence complex $[Pt(NH_3)_2(SCN)_2][Pt(NH_3)_2(SCN)_2I_2]$ (**I**). The structure of *cis*-dithiocyanatodiammine platinum(II) is known [15]. The crystals contain square-planar complexes arranged one above another in columns. The strong peak on the RDF curve at $r=4.05$ Å corresponds to the distances between Pt atoms in these columns (Fig. 1, bottom). The peak at 2.29 Å corresponds to the superposition of the contributions to the RDF from the closest Pt–S (dashed-and-dotted line) and Pt–N(NH_3) distances, 2.30 and 2.21 Å, respectively.

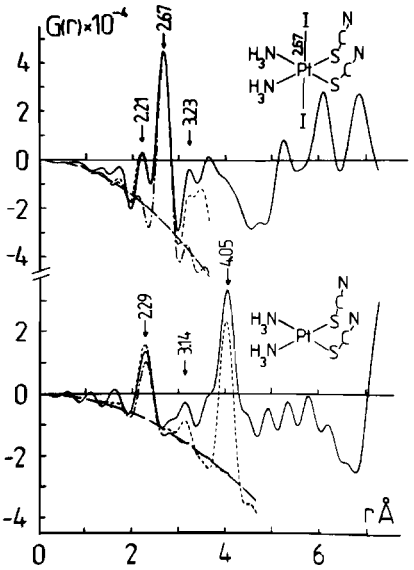

Fig. 1. RDFs for *cis*-$[Pt^{II}(NH_3)_2(SCN)_2]$ (bottom) and $[Pt^{IV}(NH_3)_2(SCN)_2I_2]$ (**III**). Solid lines are experimental RDFs. RDFs of structural models: dashed-and-dotted lines, the contribution of Pt–S distances (bottom); Pt–I (top); dashed lines, the overall contribution of the interatomic distance types mentioned below. Long dashes — reference line for absolute intensities of RDF peaks [4, 5], determined by the mean density ρ_0 (the number of stoichiometric units in Å) and chemical composition of a sample. Here and in Fig. 2 RDFs are normalized to stoichiometric units containing one Pt atom. Numbers at arrows indicate the positions of experimental RDF peaks in Å. *cis*-$[Pt^{II}(NH_3)_2(SCN)_2]$. Parameters of the structural model used for RDF simulation [4, 5]. Contributions of the distances in the order PtPt; PtS; PN(NH_3); PtC; SS; SN(NH_3): $r_{kj}=4.03$; 2.30; 2.21; 3.15; 3.23; 3.1 Å; $\sigma_{kj}=0.14$; 0.11; 0.11; 0.12; 0.12; 0.12 Å; $N_{kj}=2$; 4; 4; 4; 2; 4; $\rho_0=0.005269$ Å^{-1}. $[Pt^{IV}(NH_3)_2(SCN)_2I_2]$. PtI; PtS; PtN($NH_3$); PtC; IS; IN($NH_3$); IC; IN; SS: SN($NH_3$): $r_{kj}=2.67$; 2.29; 2.19; 3.23; 3.51; 3.45; 3.22; 3.47; 3.23; 3.2 Å; $\sigma_{kj}=0.1$; 0.11; 0.11; 0.12; 0.12; 0.12; 0.12; 0.12; 0.12 Å; $N_{kj}=4$; 4; 4; 4; 8; 8; 4; 4; 2; 4; $\rho_0=0.00425$ Å^{-3}.

Here and in Fig. 2, dashed lines show overall theoretical RDF profiles, formed by contributions of all interatomic distances taken into account in the model. When comparing this profile with experimental RDF, one should bear in mind that in a model calculation it is possible to specify quite completely only the limiting number of distance types. These are intramolecular distances within a complex whose model is constructed, as well as some substantial short intercomplex distances if the object of RDF simulation is the relative position of molecules. The latter case will take place for RDFs shown in Fig. 2. Therefore, quantitative agreement between dashed and solid lines can be expected at r up to 3–3.5 Å while at greater r the model should reproduce only semiquantitatively or qualitatively some characteristic features of RDF, such as, for example, the above-mentioned peak of PtPt distances at 4.05 Å. With increasing r, the contribution to RDF rapidly increases from more and more numerous and practically unaccountable types of distances determined by packing of molecules in crystals or amorphous bodies [4, 5].

Oxidation of Pt^{II} to Pt^{IV} followed by bonding I atoms in axial positions leads to characteristic changes in RDF (see Fig. 1, top). The column structure disappears and hence the peak at 4.05 Å vanishes. At $r=2.67$ Å, a new dominant peak appears whose intensity corresponds to the theoretical contribution of two Pt–I distances (dashed-and-dotted line) computed per one platinum atom, i.e. each Pt atom has two I neighbours. The value of the Pt^{IV}–I distance (2.67 Å) is close to the reported values [16, 17]. The contribution of Pt–S and Pt–N(NH_3) distances with a maximum at $r=2.21$ Å is seen on the left of the Pt–I peak. The shift to the left from the analogous peak at 2.29 Å on the lower curve is mainly due to overlap of Pt–S and Pt–N contributions with the oscillating wing of the strong neighbouring Pt–I peak [18] (see dashed-and-dotted line). The structure of $[Pt(NH_3)_2(SCN)_2I_2]$ has not been determined by X-ray analysis of a single crystal. Direct data of the distance spectrum, which is RDF, permit us to state definitely that the complex structure corresponds to that shown in Fig. 1. The interpretation of the RDF confirms the assignment of the 198 cm^{-1} band in the IR spectrum of diiodide **III** to the vibrations ν(Pt–I) since the RDF indicates directly Pt–I bond formation. The XPS line position corresponding to the $Pt4f_{7/2}$ electron binding energy 75.1–75.2 eV points to the Pt^{IV} oxidation state [19].

Figure 2 presents RDFs of the compounds which are the objects of the main interest in this work. Here one can see RDFs for ammonia **I** (top) and ethylenediamine $[Pt^{II}(en)(SCN)_2][Pt^{IV}(en)(SCN)_2I_2]$

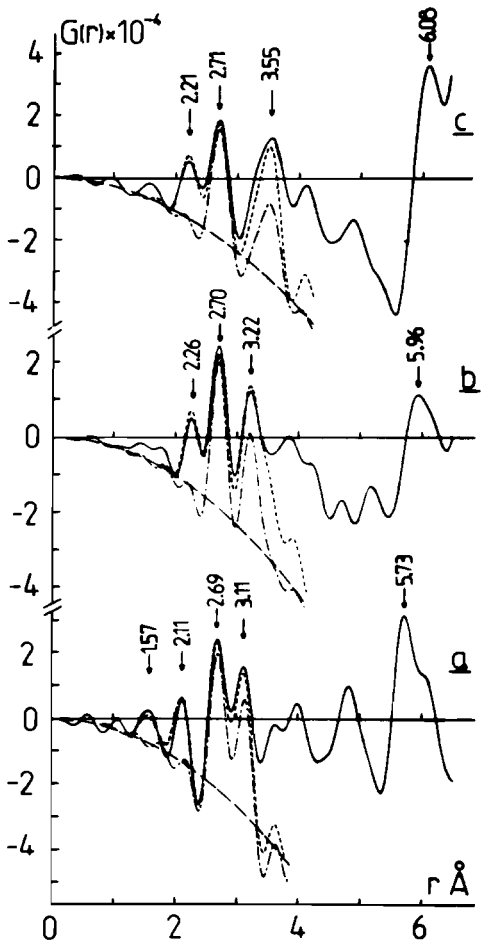

Fig. 2. RDFs for (a) $[Pt^{II}(en)_2][Pt^{IV}(en)_2I_2](ClO_4)_4$, (b) $[Pt^{II}(en)(SCN)_2][Pt^{IV}(en)(SCN)_2I_2]$, (c) $[Pt^{II}(NH_3)_2(SCN)_2][Pt^{IV}(NH_3)_2(SCN)_2I_2]$. Same as Fig. 1. Dashed-and-dotted lines, always contribution of PtI distances. The distances which give the most significant contributions to simulated RDFs are marked in Fig. 3. Model parameters: (a) PtI; $PtN(NH_2)$; $PtC(CH_2)$; $IN(NH_2)$; Cl–O; CH_2–CH_2; CH_2–NH_2: r_{kj}=2.705 and 3.10; 2.10; 2.98; 3.41 and 3.70; 1.55; 1.55; 1.55 Å; σ_{kj}=0.09 and 0.11; 0.1; 0.13; 0.12 and 0.13; 0.07; 0.07; 0.07 Å; N_{kj}=2 and 2; 8; 8; 4 and 4; 16; 4; 8; ρ_0=0.001372 Å^{-3}. (b) PtI; PtS; $PtN(NH_2)$; PtC(SCN); $PtC(CH_2)$; IS; IN; $IN(NH_2)$; IC; SS; $SN(NH_2)$; SN: r_{kj}=2.70 and 3.23; 2.33; 2.17; 3.11; 2,98; 3.52 and 3.94; 3.47 and 3.53; 3.42 and 3.85; 3.22 and 3.45; 3.23; 3.20; 2.90 Å; σ_{kj}=0.09 and 0.15; 0.13; 0.13; 0.13; 0.13; 0.13 and 0.15; 0.13 and 0.15; 0.13 and 0.15; 0.13 and 0.15; 0.12; 0.12; 0.08 Å; N_{kj}=2 and 2; 4; 4; 4; 4; 4 and 4; 2 and 2; 4 and 4; 2 and 2; 2; 4; 4; ρ_0=0.004238 Å^{-3}. (c) PtI; PtS; $PtN(NH_3)$; PtC(SCN); IC; IN; $IN(NH_3)$; IC; SS; $SN(NH_3)$; SN: r_{kj}=2.70 and 3.50; 2.26; 2.19; 3.11; 3.52 and 4.19; 3.47 and 3.47; 4.48 and 4.15; 3.22 and 3.62; 3.23; 3.20; 2.80 Å; σ_{kj}=0.1 and 0.15; 0.13; 0.13; 0.12; 0.13 and 0.15; 0.13 and 0.15; 0.13 and 0.15; 0.13 and 0.15; 0.12; 0.12; 0.08 Å; N_{kj}=2 and 2; 4; 4; 4; 4 and 4; 2 and 2; 4 and 4; 2 and 2; 2; 4; 4; ρ_0=0.004819 Å^{-3}.

(II) (middle) rhodanide complexes as well as RDF for the reference compound (bottom) of known structure $[Pt^{II}(en)_2][Pt^{IV}(en)_2I_2](ClO_4)_4$. The latter compound is a mixed-valence complex containing in crystal structure the linear chains ...I–Pt^{IV}–I...Pt^{II}...I–Pt^{IV}–I...Pt^{II}...I– with I atoms as bridges and each Pt atom surrounded by two ethylenediamine molecules in equatorial positions [16, 17]. Comparison of the RDF of this substance with the distance spectra of rhodanide derivatives allows one to demonstrate practically in a direct way the similarity of the complex structures and reveal essential differences in chain parameters caused by changes of ethylenediamine for SCN and NH_3 ligands.

At r near 2.70 Å, the RDFs of all the three complexes show Pt–I peaks. Reconstruction of their intensities and profiles shows that, in contrast to RDF of diiodide **III**, in all the cases these peaks correspond on the average to one Pt–I contact per one platinum atom. Proceeding from the model compound structure, we may conclude that half of the platinum atoms, namely Pt^{IV}, have two contacts with iodine atoms at a distance of about 2.70 Å. The decrease in the intensity of Pt^{IV}–I contribution in rhodanide complexes as compared to diiodide **III** RDF (Fig. 1, top) may be seen qualitatively if one compares 2.67 and 2.70 Å peak intensities with the intensity of the peak of the distances from Pt atoms to the equatorial ligands N and S which are the same for all the cases. The last peak is always seen on the left of the peak under discussion. The more pronounced resolution of the mentioned peaks on the lower curve can be explained mainly by the absence of Pt–S contribution at $r \approx 2.3$ Å, which shifts the peak of the distances from Pt to equatorial ligands to the right on the two upper curves. In accordance with the RDF, the IR spectrum of ammonia complex **I** shows an intense band at 189 cm^{-1} with a shoulder at 182 cm^{-1}, which can be attributed to ν(Pt–I). A slight shift of this band from 198 cm^{-1} in the spectrum of diiodide **III** appears to be due to transition from the end I atom to the bridge one in the chain ...I–Pt^{IV}–I...Pt^{II}...I–Pt^{IV}–I...Pt^{II}...I–.

The most striking evidence for chain order of heavy atoms is the appearance of new peaks on RDFs to the right of 2.7 Å peaks, the intensities of the new peaks being approximately of the same magnitude as the intensities of the peaks at 2.7 Å. Pt^{II}...I distances manifest themselves here directly, which is confirmed by model simulations of all RDFs. Dashed-and-dotted curves in Fig. 2 represent the contributions of PtI type distances in mixed-valence complex chains shown by schemes in Fig. 3. The left-hand components of the doublets are everywhere the already discussed contributions of Pt^{IV}–I dis-

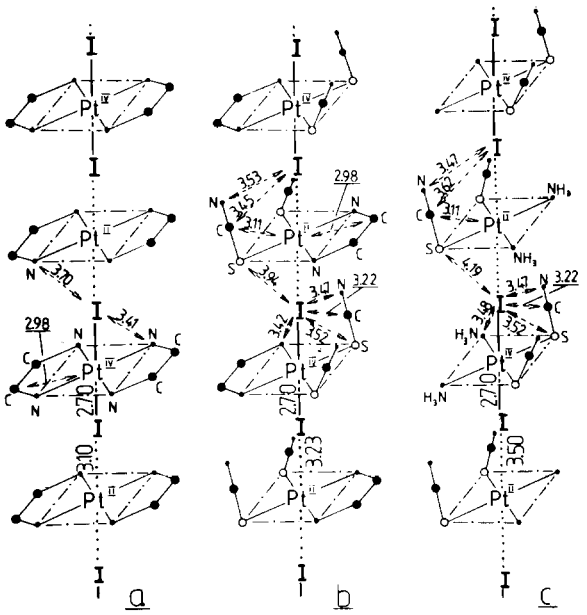

Fig. 3. Arrangement of Pt^{II} and Pt^{IV} complexes in chains with I bridges. Variants (a), (b), (c) correspond to Fig. 2. Some important distances in the models are marked. The planes containing equatorial ligands S and N surrounding Pt atoms are perpendicular to the line ...I–Pt^{IV}–I...Pt^{II}...I–Pt^{IV}–I...Pt^{II}...I–.

tances. The right-hand components correspond to Pt^{II}...I distances in the chains and exhaust the larger parts of the intensities of experimental peaks at 3.11, 3.22 and 3.55 Å. The rest of the area under the curves in the vicinity of the above-mentioned r values is mainly the contribution of quite numerous distances from Pt and I atoms to light ligand atoms. Distances important for simulation of RDF are marked in Fig. 3 and are involved in model RDF calculations.

Dashed lines in Fig. 2 correspond to the overall contribution of all distances. For the lower curve, the difference between the dashed and dashed-and-dotted lines in the range of Pt^{II}...I distances is small and the necessity of Pt^{II}...I contribution for interpreting the 3.11 Å peak is undoubtful. The two other curves show more considerable difference caused by the appearance of SCN ligands in the complexes. In both cases the full model curve (dashed) fits well the experimental one. The intensity excessive over that presented by the dashed-and-dotted Pt^{II}...I peak is in the main due to the contributions from the I...S ('half-heavy' sulfur atom) distances, as well as, to a some lesser extent, from I...C and I...N distances at $r \approx 3.1$–3.5 Å. Analogous types of distances are absent in the reference compound. Nevertheless, calculations show that it is the contribution of Pt^{II}...I distances that determines the position and high intensity of the peaks under discussion. Without this contribution it is impossible to exhaust their intensities. No other geometrically admissible arrangement of complexes without approaching Pt^{II} and I atoms in a linear chain can give such a great number of other types of interatomic distances, each having lower weight in RDF, to compensate the absence of Pt^{II}...I contribution of a pair of heavy atoms.

Thus, the analogy between the interatomic distance spectra confirms directly the similarity between the structures of the three compounds. However, there is a significant quantitative difference in their Pt^{II}...I distances. In the reference ethylenediamine complex, this distance is 3.10 Å which is consistent with reported data [16, 17] within the accuracy and resolution limits of RDF method and discrepancy in single crystal X-ray analysis data. In **II**, after changing one of the ethylenediamine molecules for two SCN groups this distance increases to 3.23 Å. Finally, in **I**, change of the second ethylenediamine molecule for ammonia ligands results in an even larger increase of Pt^{II}...I distance up to 3.50 Å. In all cases, the Pt^{IV}–I distance is constant and equals 2.70 Å. Increased Pt^{II}...I distance means a more weak coupling of Pt^{II} and Pt^{IV} complexes in chains. The same also confirms the increase in $\sigma(Pt^{II}...I)$, the r.m.s. deviation from an average distance $r(Pt^{II}...I)$. In going from the reference complex to rhodanide complexes, the $\sigma(Pt^{II}...I)$ value increases from 0.11 to 0.15 Å while $\sigma(Pt^{IV}–I)$ in all iodine complexes including diiodide **III** (Fig. 1) is nearly constant 0.09–0.1 Å. Pt^{IV}–I bond strength is approximately constant for all the compounds and this corresponds to approximately equal amplitudes of atomic vibrations along the bond direction. The weakened interaction between Pt^{II} and I atoms leads to increased vibration amplitude and perhaps to appearance of some statistically slightly different distances between Pt^{II} and Pt^{IV} complexes.

The described facts can be interpreted as a consequence of iodine atom bridge function weakening in this series of compounds and, as a result, of decrease of electron delocalisation in the chain ...I–Pt^{IV}–I...Pt^{II}...I–Pt^{IV}–I...Pt^{II}...I–. A similar interpretation of relative increase in Pt^{II}...halogen distances for a series of I, Br and Cl bridges has been given for chain structures [16]. The decrease in delocalization of electrons correlates with significant increase in the along-chain charge transfer band maximum frequency $\nu(Pt^{II} \Rightarrow Pt^{IV})$ from 14 000 to 18 200 cm^{-1} [2] in going from the reference ethylenediamine complex with short $r(Pt^{II}...I)$ to the dithiocyanatodiammine complex **I** with long $r(Pt^{II}...I)$.

Concerning the question on approximating platinum oxidation number in chains like those under study to the average 3+ [20], it is interesting to

note that already in the first work on the synthesis of **I** [1] the ESR signal ($g_{eff}=2.18$) had been detected. This signal indicates the presence of a Pt^{III} state with some statistical weight in the substance. We have detected the ESR signal ($g=2.2$ and 2.3) for the reference complex $[Pt^{II}(en)_2][Pt^{IV}(en)_2I_2](ClO_4)_4$ as well. The g factor values indicate that this signal is also produced by Pt^{III} [21]. In both cases the signals are rather weak and it cannot be excluded that we observe not all but only the most strong narrow lines. In the latter case the signal intensity is approximately by an order of magnitude greater than in the former case, that points to the greater weight of Pt^{III} state. Signal intensity decay and consequently lowering the fraction of Pt^{III} state with increasing $Pt^{II}...I$ distance is consistent with the conclusion about decreased electron delocalization in the chain $...I–Pt^{IV}–I...Pt^{II}...I–Pt^{IV}–I....Pt^{II}...I–$ in compound **I** relative to the reference complex. Thus all the data show that in rhodanide complexes, particularly in the ammonia derivative, Pt^{II} and Pt^{IV} oxidation states are pronounced more definitely than they are in a compound wherein equatorial positions of the platinum atom are completely occupied by ethylenediamine.

Returning to discussing the structural models of complexes, in connection with RDF data, we can note additional evidence for the linear disposition of Pt and I atoms. Very strong peaks locating on the right of the discussed ones appear at r values close to the sum of the distances Pt^{IV}–I and $Pt^{II}...I$ (5.73, 5.96 and 6.08 Å). Qualitatively these peaks correspond to $Pt^{II}...Pt^{IV}$ separations along the chains in which every Pt atom has two Pt neighbours at these distances. Unfortunately, in this range of r values, quantitative simulation of RDF is impossible owing to the significant contribution of intermolecular distances [4, 5].

A few words about location of SCN ligands in the complexes. Model simulations of RDF profiles in Fig. 2, showed the contribution of Pt...C distances from platinum atoms to rhodanide ligand carbons to be rather substantial. According to results of fitting model and experimental RDFs, these distances are taken to be equal to 3.11 Å. From this value one can estimate the angle between the Pt–S bond and S–C–N line using average r(Pt–S) = 2.33 and 2.26 Å obtained in reconstructions of RDFs of ethylenediamine **II** and ammonia **I** complexes in Fig. 2 and r(S–C) = 1.55 Å [15]. The angle equals 105 and 108° for **II** and **I**, respectively. These values are very close to the average value of this angle 108° in *cis*-dithiocyanatodiammine platinum(II) [15, 22]. A sufficiently accurate estimation of the inclination of the rhodano group towards the plane of equatorial surroundings of platinum presents difficulties since the contributions of I...C and I...N distances depending on this angle are less important for RDF peak shape. Therefore these distances can be found with larger ambiguity than Pt...C ones. We can note only that this angle is significantly smaller than 70° in *cis*-$[Pt(NH_3)_2(SCN)_2]$ [15, 22], which follows from inadmissibility of too close contacts of C and N atoms with the I atom attached to Pt^{IV} in axial position.

Note in conclusion that all interatomic distances accepted in fitting simulated and experimental RDFs are physically reasonable, consistent with typical crystallochemical data on bond lengths and bond angles, and correspond to the structures, which can be realized without spatially impossible arrangement of atoms. A relatively large number of distances taken into account, i.e. the multiplicity of simulation parameters (see captions for Figs. 1 and 2), should not give rise to doubt in our case. First, these distances can be readily divided into groups essential for reconstruction of peaks in different ranges of r values. In other words, a reasonable number of model contributions is typically placed under each RDF peak. Besides, in systems containing heavy atoms there are always peaks of a dominant intensity which are decisive for choosing a given model, other peaks being a background. Second, many distances are not independent. For example, all distances from the I atom to equatorial ligands and to C and N atoms of SCN groups are determined by unambiguously measured Pt^{IV}–I and $Pt^{II}...I$ distances as well as by location of a linear SCN group with known bond lengths between its atoms.

References

1 G. S. Muraveiskaya, G. M. Larin and V. F. Sorokina, *Zh. Neorg. Khim., 13* (1968) 1466.
2 R. J. H. Clark and M. Kurmoo, *J. Chem. Soc., Dalton Trans.,* (1980) 524.
3 R. J. H. Clark, M. Kurmoo, K. D. Buse and H. J. Keller, *Z. Naturforsch., Teil B, 35* (1980) 1272.
4 V. I. Korsunsky, *J. Organomet. Chem., 311* (1986) 357.
5 V. I. Korsunsky, *Zh. Strukt. Khim., 28* (N1) (1987) 80.
6 V. I. Korsunsky, *Zh. Neorg. Khim., 34* (1989) 139.
7 V. I. Korsunsky, G. S. Muraveiskaya and V. E. Abashkin, *Zh. Neorg. Khim., 33* (1988) 669.
8 V. I. Korsunsky, T. A. Fomina and N. N. Chalisova, *Zh. Neorg. Khim., 33* (1988) 2594.
9 A. F. Skryshevskii, *Structural Analysis of Liquids and Amorphous Bodies,* Visshaya shkola, Moskow, 1980 (in Russian).
10 B. E. Warren, *X-ray Diffraction,* Addison Wesley, Reading, MA, 1969, Ch. 10, p. 116.
11 A. A. Grinberg, Izv. Inst. *Izucheniyu Platiny, 6* (1928) 122.

12 G. S. Muraveiskaya, V. F. Sorokina and I. I. Chernyaev, *Proc. IX Conf. Coordination Chemistry, Tashkent, 1968*, p. 87 (in Russian).
13 O. Becaroglu, H. Breer, H. Enders, H. J. Keller and H. N. Gung, *Inorg. Chim. Acta, 21* (1977) 183.
14 G. S. Muraveiskaya, A. A. Sidorov, G. N. Emelyanova and E. M. Trishkina, *Zh. Neorg. Khim., 35* (1991) in press.
15 Ya. Ya. Bleidelis, *Kristallografiya, 2* (1957) 278.
16 N. Matsumoto, M. Yamashita and S. Kida, *Acta Crystallogr., Sect. B, 35* (1979) 1458.
17 H. Enders, H. J. Keller, R. Martin, H. N. Gung and U. Traeger, *Acta Crystallogr., Sect. B, 35* (1979) 1885.
18 V. I. Korsunsky, *Zh. Strukt. Khim., 26* (N2) (1985) 75.
19 V. I. Nefedov and Ya. V. Salyn, *Inorg. Chim. Acta, 28* (1978) L135.
20 M. Yamashita, N. Matsumoto and S. Kida, *Inorg. Chim. Acta, 31* (1978) L381.
21 N. Matsumoto and T. Watanabe, *J. Am. Chem. Soc., 108* (1986) 1308.
22 G. A. Kukina, *Zh. Strukt. Khim., 3* (1962) 474.